Effects of Dispersed Phase Composition on Thermoplastic Polyolefins

M. H. Ha,[1,*] B. K. Kim,[1] E. Y. Kim[2]

[1]*Department of Polymer Science and Engineering, Pusan National University, Pusan 609-735, Korea*
[2]*Research Institute of Industrial Technology, Pusan National University, Pusan 609-735, Korea*

Received 8 July 2003; accepted 31 January 2004
DOI 10.1002/app.20447
Published online in Wiley InterScience (www.interscience.wiley.com).

ABSTRACT: Ternary blends of polypropylene (PP), ethylene–octene copolymer (mPE), and high-density polyethylene (HDPE) were prepared based on the phase behavior and physical properties of mPE/HDPE binary blends, and the results were interpreted in terms of morphology and both rheological and mechanical properties of the ternary blends as well as the binary blends. It was found that when mPE encapsulates HDPE in the PP matrix, compared to the encapsulation of mPE by HDPE, better blend properties were obtained, presumably because of the compatibilizing effect of mPE between PP and HDPE. © 2004 Wiley Periodicals, Inc. J Appl Polym Sci 93: 179–188, 2004

Key words: blends; phase behavior; ethylene–octene copolymer (mPE); high-density polyethylene (HDPE); polypropylene (PP)

INTRODUCTION

Because of its easy processing, low cost, and good thermal and mechanical properties, isotactic polypropylene (PP) has been widely used as a commodity polymer. However, because of its poor impact strength at low temperature, PP has been blended with various elastomers to improve its toughness. It is generally known that the toughness of PP can be improved by addition of elastomer but such mechanical properties as stiffness, hardness, and heat distortion temperature are decreased upon blending. To improve such mechanical properties, inorganic fillers including talc, glass fiber, $BaSO_4$, and $CaCO_3$, for example, have been incorporated in PP/elastomer blends. The control of microstructure is a very important factor for determination of physical properties of multicomponent blends. Most works on polyolefin blends have investigated binary blends[3–8] with ethylene–propylene copolymer (EPR) and ethylene–propylene–diene terpolymer (EPDM), although investigations of polyolefin ternary blends are rare.[9–15]

In this work, we used an ethylene–octene copolymer (mPE) for impact modifier of PP. The physical and rheological properties and morphology of PP/mPE/HDPE ternary blends were investigated to study the effects of mPE/HDPE binary composition. The effects of mPE content on mPE/HDPE binary blends were also examined to understand more clearly the effects of mPE/HDPE binary composition on PP/mPE/HDPE ternary blends.

EXPERIMENTAL

Materials

PP and HDPE used in this experiments were commercial grades produced by Korea Petrochemical Co. Ltd. (Ulsan, Korea): Polypropylene and HDPE (melt flow rates of 8.1 and 0.3 g/10 min, respectively) were used for blending. The ethylene–octene copolymer used was Engage 8200 (24 wt % 1-octene contents and density 0.870 g/cm^3; DuPont Dow Elastomers, Wilmington, DE). Important characteristics of the materials are listed in Table I.

Preparation of polymer blending

Blends were prepared by an Ikegai corotating twin-screw extruder (PCM-45, Kawasaki, Japan) with screw diameter 45 mm, L/D = 32, at 220 rpm and 230°C. The mPE/HDPE binary blends were prepared at 33.3/66.7, 50/50, 66.7/33.3, and 83.3/16.7 wt % and these master pellets were used to prepare the PP/mPE/HDPE ternary blends. PP and mPE/HDPE master pellets were mixed at 70/30 wt %: The compositions of PP/mPE/HDPE ternary blends were 70/10/20, 70/15/15, 70/20/10, and 70/25/5. For reference purposes, 70/30 wt % PP/mPE and PP/HDPE binary blends were also prepared with the same extruding condition of ternary blends.

**Present address:* R&D Center, Korea Petrochemical Co. Ltd., Ulsan, Korea.
Correspondence to: B. Kim (bkkim@pnu.edu).

TABLE I
Characteristics of Test Materials

Sample	MFR[a] (g/10 min)	Density (g/cm^2)	M_w ($\times 10^5$ g/mol)	Viscosity at 100 rad/s	Source
PP	8.1	0.90	2.53	3355.6	4017, Korea Petrochemical Ind. Co.
HDPE	0.3	0.962	1.61	13,739.0	B502, Korea Petrochemical Ind. Co.
mPE	5.0	0.870	—	4001.3	Engage 8200, DuPont Dow Elastomers, Octene 24%

[a] PP: MFR is measured under 2.16 kg at 230°C; HDPE and mPE: MFR is measured under 2.16 kg at 190°C.

Characterizations

Injection-molded samples were made by a Nissei (Hyogo, Japan) 35-oz. injection-molding machine at 230°C cylinder temperature and 40°C mold temperature to analyze mechanical properties. The tensile properties and flexural modulus were measured with an Instron 4301 (Poole, UK). The mechanical properties were measured according to the corresponding ASTM method.

The rheological properties were measured by an advanced rheometrics expansion system (ARES; Rheometric Scientific, Piscataway, NJ) at 230°C with a 25-mm parallel-plate fixture at a constant strain of 15% and oscillatory angular frequency ranging between 0.1 and 500 rad/s.

The morphology of dispersed phase was analyzed by a JEOL JSM-820 scanning electron microscope (JEOL, Tokyo, Japan). The fracture surfaces were prepared by breaking compression-molded samples in liquid nitrogen. The surface was etched for 3 min in boiling *n*-heptane to remove the ethylene–octene copolymer, followed by coating with gold.

RESULTS AND DISCUSSION

HDPE/mPE binary blends

Rheological properties

Complex viscosities (η^*) of HDPE, mPE, and their blends are shown in Figure 1. Values of η^* of all samples showed shear thinning behavior and viscosity functions of HDPE/mPE binary blends are located between those of the two neat components.

Utraki et al.[16] divided viscosity–composition curve into three types: positive-deviation blend (PDB); negative-deviation blend (NDB); and positive-negative-deviation blend (PNDB). Values of η^* versus blend composition for HDPE/mPE binary blends are shown in Figure 2. The viscosity–composition curves of HDPE/mPE binary blends exhibited PNDB at low frequencies ($\sim$ 10 rad/s) and exhibited NDB above 10 rad/s.

The inflection point of the viscosity–composition curve in HDPE/mPE binary blends moved to higher HDPE content with increasing frequency. Assuming phase inversion occurs at the inflection point,[17] the less-viscous phase shows a greater tendency to be the continuous phase.[2]

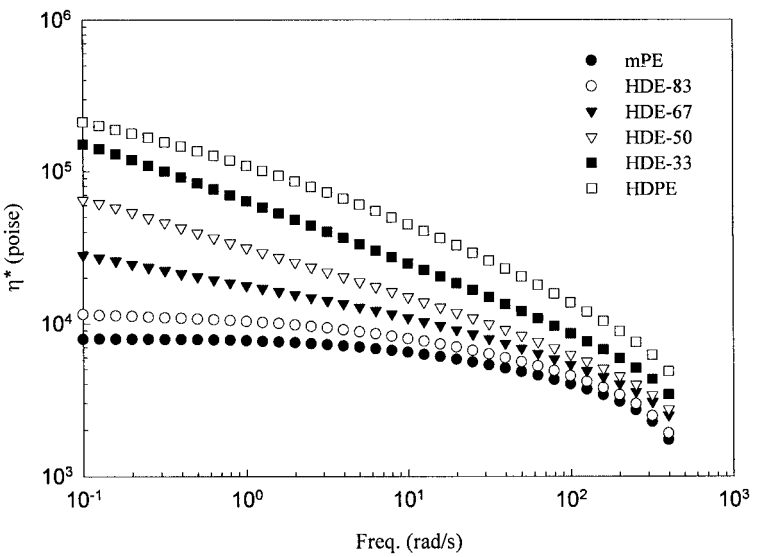

Figure 1 Complex viscosities for HDPE, mPE, and HDPE/mPE blends at 230°C

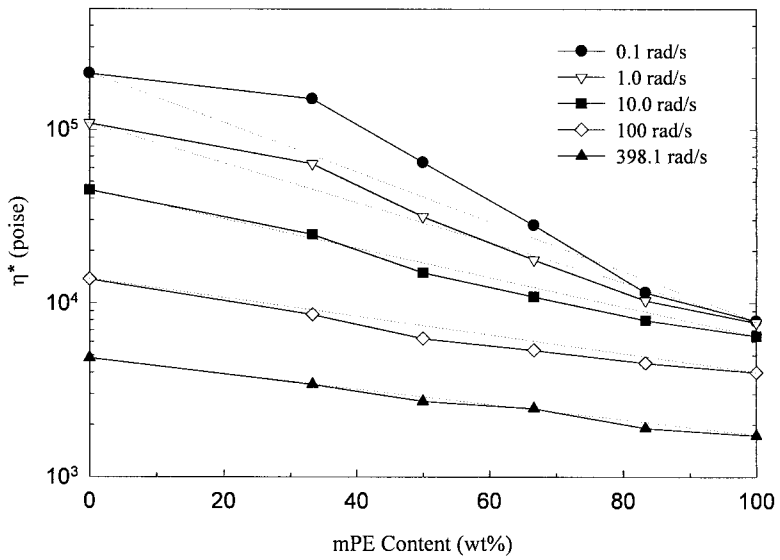

Figure 2 Plots of η^* versus blend composition in HDPE/mPE blends at 230°C.

The Cole–Cole plots of HDPE/mPE binary blends are shown in Figure 3. The semicircles are observed for HDPE, mPE, HDE-33, and HDE-83 but not for HDE-50 and HDE-67. A drift from the semicircle is seen at low frequencies for HDE-50 and HDE-67. The deviation is largest for HDE-67. Wisniewski et al.[20] observed that this drift does not appear for homopolymer and compatible polymer blends, but does appear for incompatible blends at low frequencies. Valenza et al.[21] observed the same type of Cole–Cole plots in Nylon 12/PP/compatibilizer blends as we observed in HDPE/mPE binary blends. They interpreted that the shape of the Cole–Cole plot was influenced by particle size of dispersed phase and interphase effects. Montfort et al.[22] reported a double-relaxation phenomenon of the Cole–Cole plots in two polystyrene fractions blends having different molecular weights. Each relaxation was attributed to the prevailing action of one of the two components of the blends. Graebling et al.[23] reported the relaxation at high frequencies stands for matrix and at low frequencies stands for relaxation of dispersed phase. Based on the above reports, HDPE/mPE binary blends could be compatible depending on the composition. Following Graebling et al., the major components of HDE-83 and HDE-33 are mPE and HDPE, respectively. The is, the matrix of HDE-83 is mPE and that of HDE-33 is HDPE. Therefore HDE-50 and HDE-67 may have cocontinuous phase morphology in the melt.

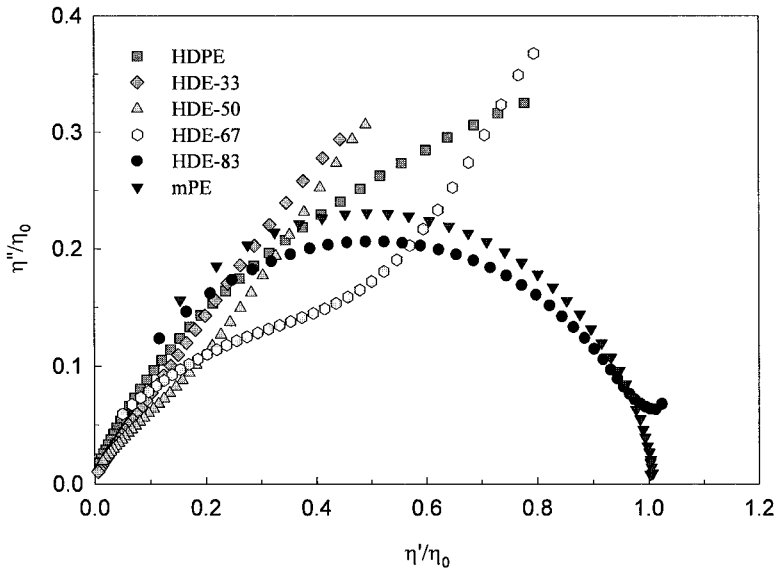

Figure 3 Cole–Cole plots for HDPE, mPE, and HDPE/mPE binary blends at 230°C.

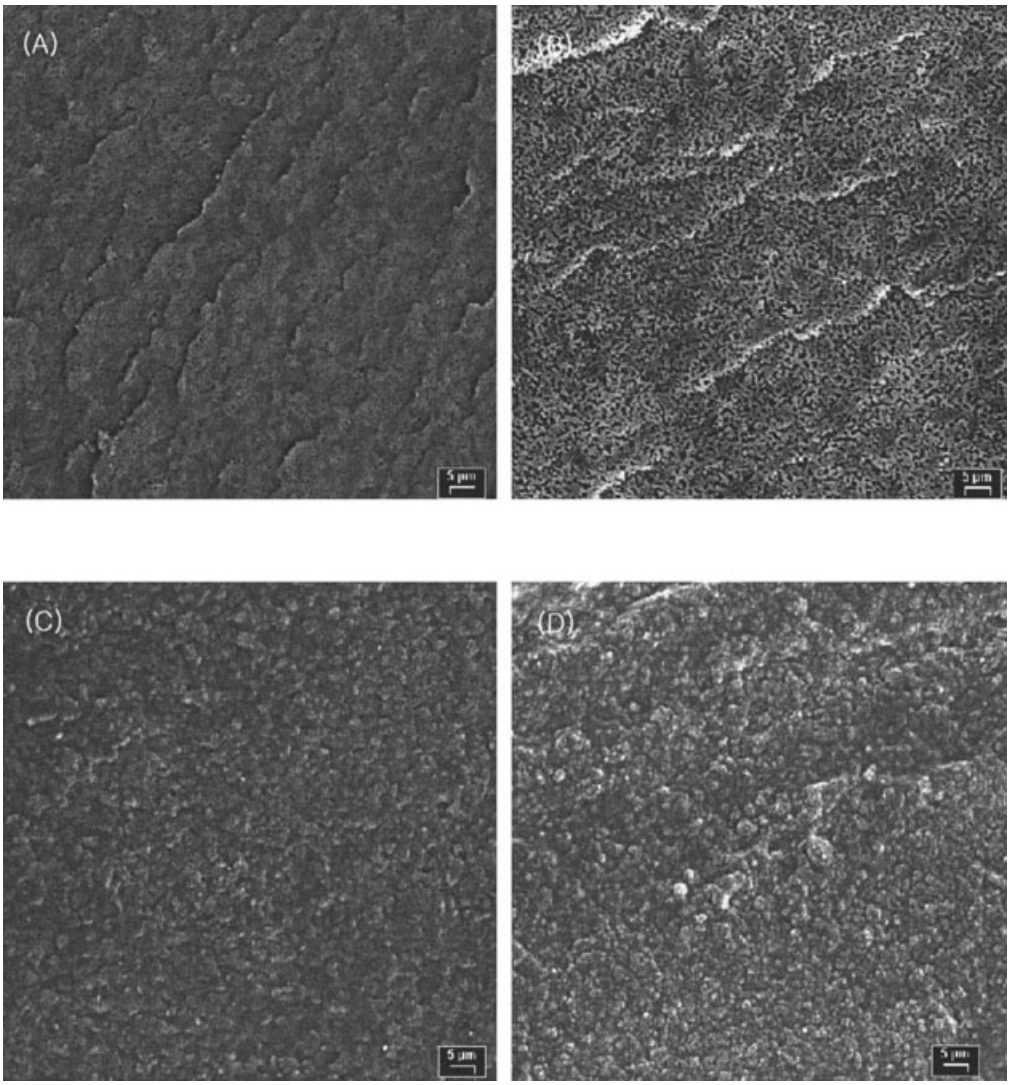

Figure 4 SEM micrographs of HDPE/mPE binary blend systems (×1000): (A) HDPE/mPE (66.7/33.3); (B) HDPE/mPE (50/50); (C) HDPE/mPE (33.3/66.7); (D) HDPE/mPE (16.7/83.3).

Morphology

Compression-molded samples were used to observe SEM morphology of binary blends. The morphologies of HDPE/mPE binary blends are shown in Figure 4. HDE-33 and HDE-50 show spherical droplets of mPE embedded in the HDPE matrix, but HDE-67 and HDE-83 show HDPE droplets embedded in the mPE matrix (Fig. 4). These SEM morphologies are in agreement with the results of rheological observations.

Physical properties

The stress–strain curves of HDPE/mPE binary blends are shown in Figure 5. The yield points of blends were observed above 50 wt % HDPE contents. Tensile strength, elongation at break, and Young's modulus with varying compositions are shown in Figures 6 and 7, respectively. As expected, Young's modulus and tensile strengths at yield and break decreased with increasing mPE content. Young's modulus–composition curve exhibited monotonically decreasing NDB. The slope of Young's modulus–composition curve decreased rapidly up to 50 wt % mPE, and slowly above 66.7 wt % mPE contents. The elongation at break shifted suddenly between 33.3 and 50 wt % of mPE content, indicative of phase inversion at this composition. The elongation and tensile strength at break of mPE were not measured because the sample was not broken within the limit of measurements.

PP/mPE/HDPE ternary blends

Rheological properties

Values of η^* for PP, PP/mPE, and PP/HDPE binary blends and PP/mPE/HDPE ternary blends are shown in Figure 8. Viscosity yields are seen at 0.1–1.0 rad/s

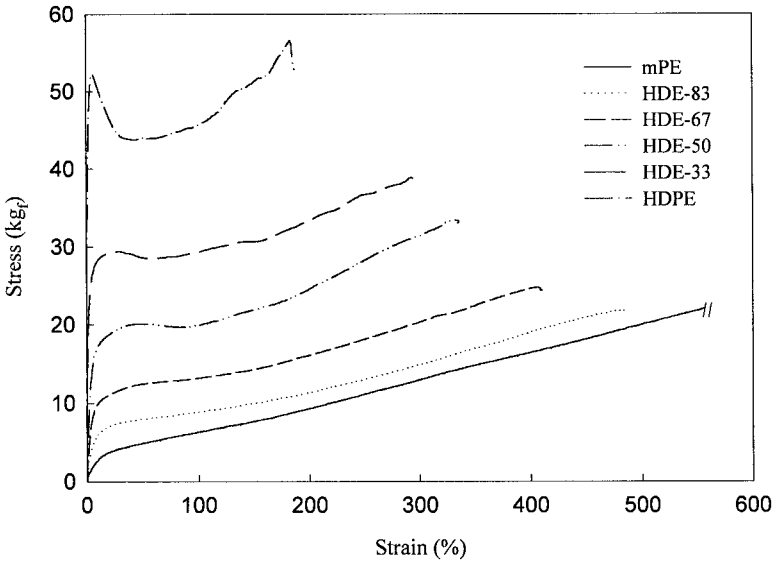

Figure 5 Stress–strain curves for HDPE, mPE, and HDPE/mPE binary blends.

for PHE-20, PHE-25, and PPE-30 blends. Viscosity yield increased with increasing mPE contents, and was not observed with <15 wt % mPE because of the insignificant particle interactions.

Relationships of η^* versus composition are shown in Figure 9. η^*–composition curves of PP/mPE/HDPE ternary blends, having a minimum at PHE-25, exhibited NDB type at all frequencies. NDB with minimum was observed when the viscosity of dispersed phase was much higher than that of the continuous phase.[17] The viscosity of the PP matrix is lower than that of the dispersed phase of HDPE/mPE blends, as well as HDPE in this study.

The Cole–Cole plots of PP/mPE/HDPE ternary blends are shown in Figure 10. The Cole–Cole plots of PPH-30, PHE-10, and PHE-15 are semicircular and those of PHE-20, PHE-25, and PPE-30 show double relaxations, which are consistent with the phase inversion point of the HDPE/mPE blend.

Morphology

SEM micrographs of PPH-30 and PPE-30 and all ternary blends are shown in Figure 11. The morphology of all ternary blends shows that the HDPE droplets are encapsulated by mPE, which are embedded in the PP matrix. For PHE-10, not all of HDPE particles are encapsulated by mPE because of insufficient mPE to surround HDPE droplets. The morphology of PHE-25

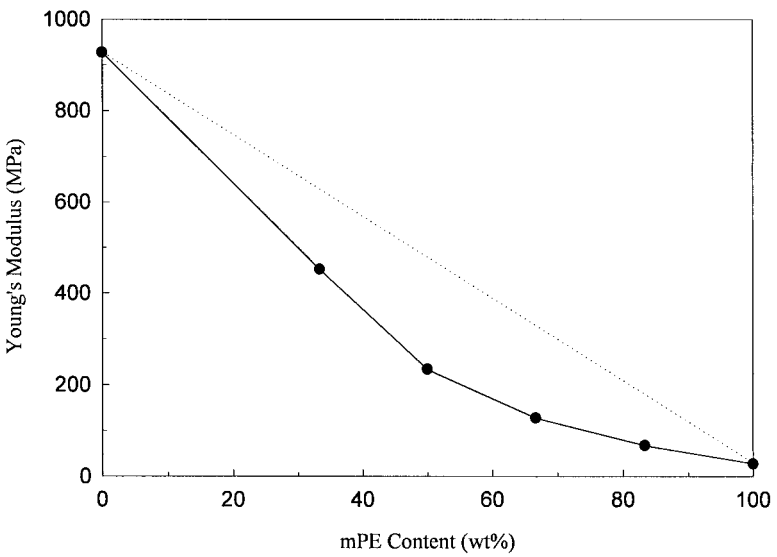

Figure 6 Young's modulus versus composition in HDPE/mPE blends.

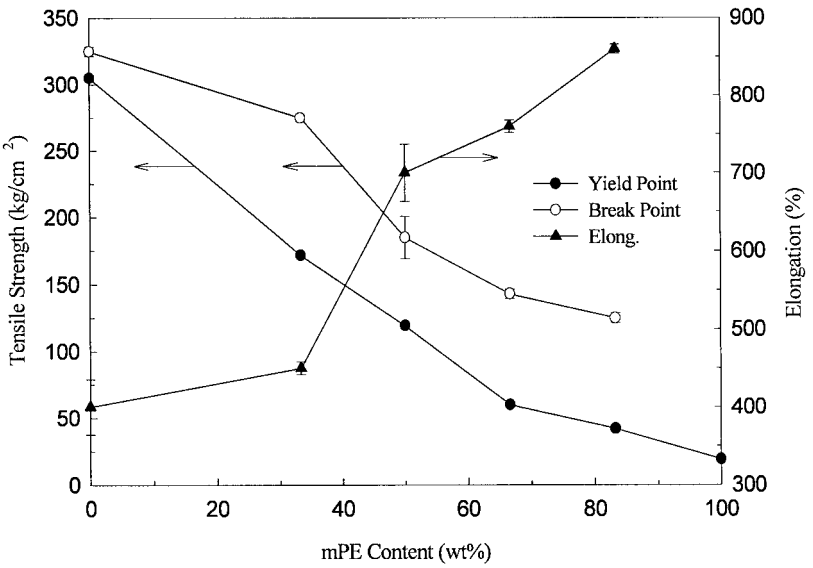

Figure 7 Tensile strength at yield and break and elongation at break versus blend composition in HDPE/mPE blends.

is similar to that of PPE-30. The extent of encapsulation in ternary blends is increased with increasing mPE concentration and the requirement for complete encapsulation seems to be >83 wt % mPE in HDPE/mPE binary blends in our study.

The particle sizes of PP/mPE/HDPE ternary blends decreased with decreasing viscosity of HDPE/mPE, that is, decreasing the viscosity ratio of the dispersed phase (HDPE/mPE) to the PP matrix. For PPE-30, although the viscosity ratio of mPE to PP is closer to unity than that for any other components, the particle size is larger than that of PHE-20 and PHE-25. Larger particles in PPE-30 are presumably obtained because of the easier coalescence of droplets during compression molding, compared with that of PHE-20 and PHE-25.

Physical properties

Mechanical properties are summarized in Table II. The dependency of physical properties of ternary blends on composition of HDPE/mPE binary blends

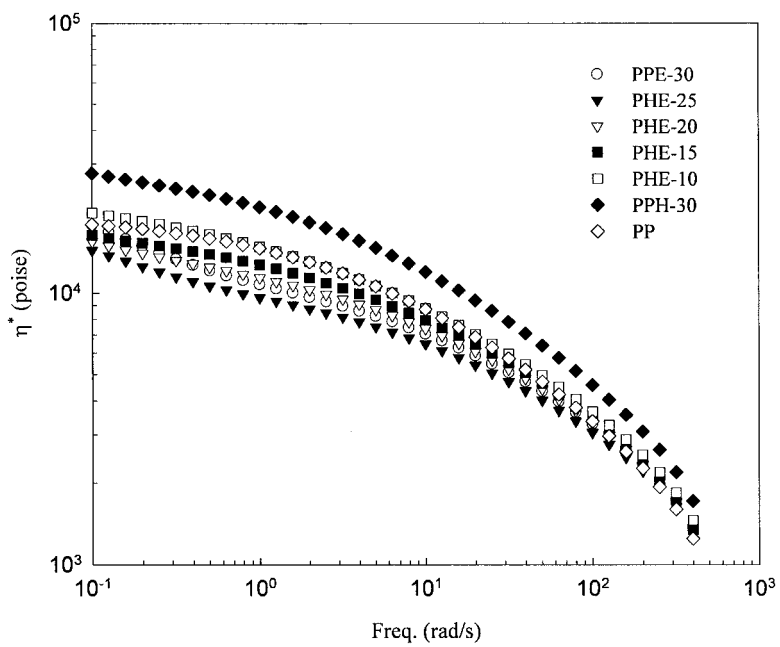

Figure 8 Complex viscosities for PP/PP/mPE (70/30), and PP/HDPE (70/30) binary blends and PP/mPE/HDPE ternary blends at 230°C.

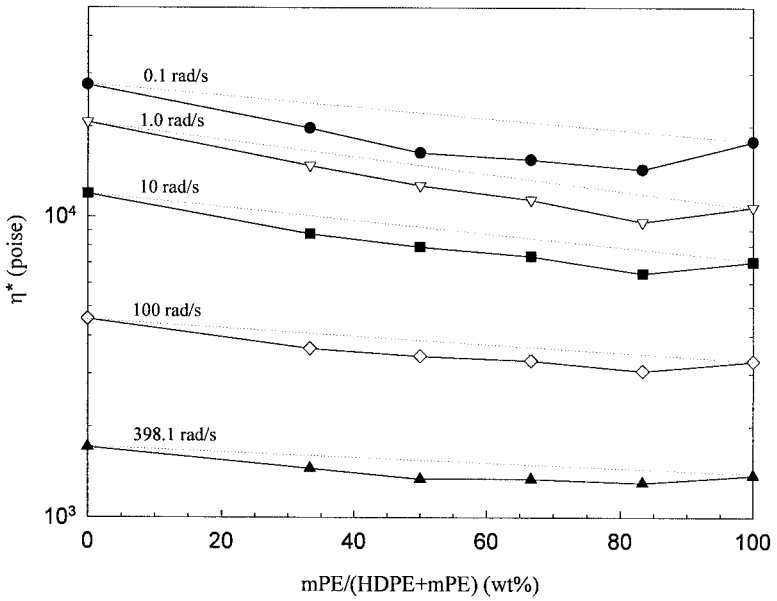

Figure 9 Plots of η^* versus HDPE/mPE binary composition in the PP/mPE/HDPE ternary blends at 230°C.

is shown in Figure 12 and Figure 13. Yield strength and hardness, showing PDB, monotonically decreased with increasing mPE content of HDPE/mPE blends. Tensile strengths of HDPE/mPE blends exhibit NDB. The dependency of Izod impact strength, flexural modulus, and elongation at break on binary composition exhibits PNDB. The slope of the flexural modulus–composition curve decreases slowly with increasing mPE contents and the greatest decrease was seen between PHE-25 and PPE-30, which provides evidence that mPE is reinforced by HDPE forming cocrystallization. As known in Figure 11, the particle size rapidly decreased between PHE-15 and PHE-20, so that the Izod impact strength at 23°C suddenly increased at those compositions. This is in substantial agreement with results reported by Wu,[23] who claimed brittle–ductile transition occurred abruptly at the critical particle diameter of the dispersed phase. Stehling et al.[15] claimed that in the case of PP-rich blends, increasing the HDPE volume fraction above 50%, at constant total elastomer level, caused a sharp decline in impact strength (unnotched, at −29°C) in the PP/EPR/HDPE ternary blends. In our work, mPE can be replaced by HDPE without any loss of notched impact strength, so long as HDPE constituted no more

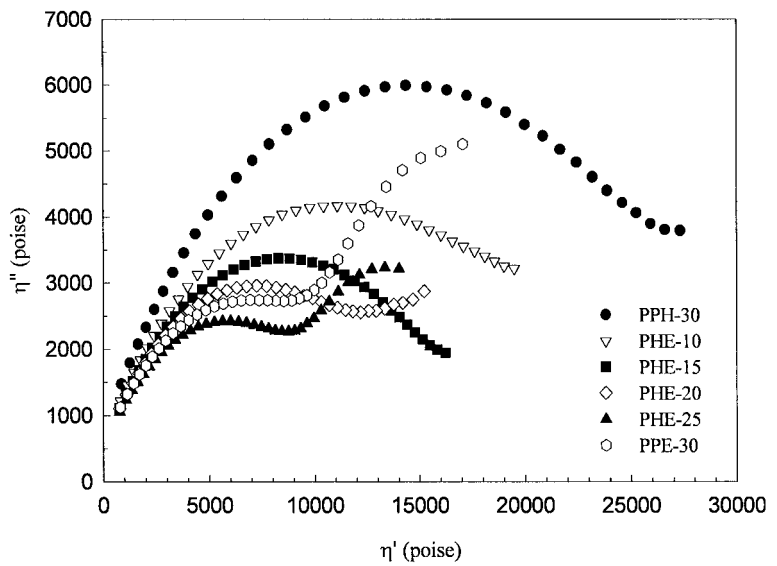

Figure 10 Cole–Cole plots for PP/HDPE, PP/mPE binary, and PP/mPE/HDPE ternary blends at 230°C.

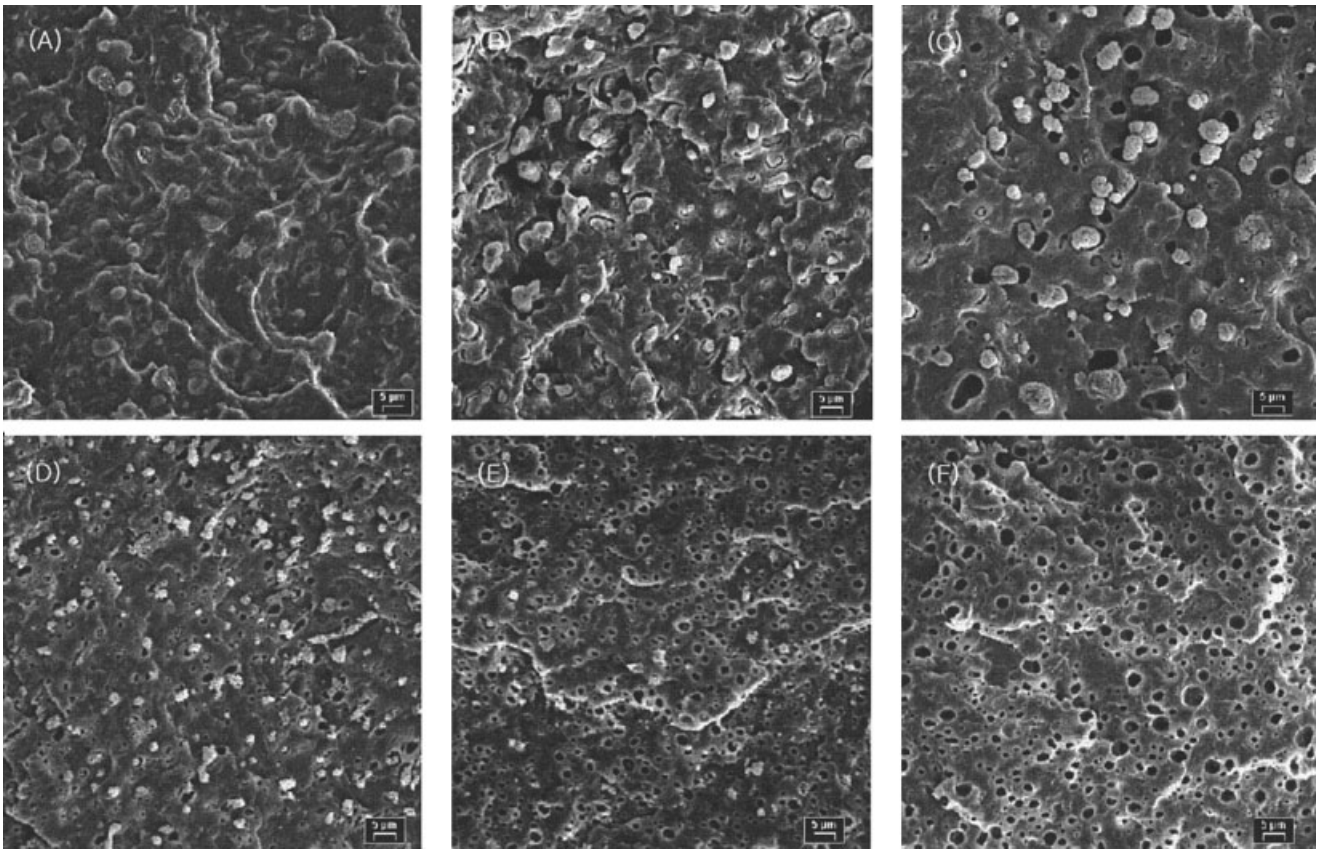

Figure 11 SEM micrographs of PP/HDPE, PP/mPE, and PP/mPE/HDPE blends (×1000): (A) PP/HDPE (70/30); (B) PP/mPE/HDPE (70/10/20); (C) PP/mPE/HDPE (70/15/15); (D) PP/mPE/HDPE (70/20/10); (E) PP/mPE/HDPE (70/25/5); (F) PP/mPE (70/30).

TABLE II
Mechanical Properties of Base Polymers and Their Blends

Sample series	Sample	Melt flow rate at 230°C (g/10 min)	Tensile strength at Yield (kg_f/cm^2)	Tensile strength at Break ($kg/cm_f/cm^2$)	Tensile strength Elong. (%)	Flexural modulus (kg_f/cm^2)	Young's modulus (kg_f/cm^2)	Izod impact strength (kg_f/cm) 23°C	Izod impact strength (kg_f/cm) 0°C	Rockwell hardness (R Scale)
Base polymer	PP	8.1	375	410	560	18,000	—	2.1	1.4	105
	HDPE	0.3[a]	305	325	400	10,900	9270	83.8	85.1	54
	mPE	5.0[a]	19	—	>1000	—	280	—	—	—
Binary blend	HDE-83	4.5[a]	42	125	860	—	675	—	—	—
	HDE-67	3.4[a]	60	143	760	—	1275	—	—	—
	HDE-50	2.3[a]	119.3	185	700	—	2340	—	—	—
	HDE-33	1.1[a]	171.7	275	450	—	4520	—	—	—
	PPE-30	9.8	220	275	490	9,200	—	40.3	31.5	58
	PPH-30	5.2	365	8	560	18,300	—	2.8	2.2	96
Ternary blend	PHE-25	11.0	260	310	550	11,500	—	47.8	31.9	70
	PHE-20	9.1	275	320	580	11,900	—	46.8	13.7	73
	PHE-15	8.9	300	120	660	12,900	—	9.0	5.0	82
	PHE-10	7.2	330	25	270	14,400	—	6.3	4.1	87

[a] MFR is measured under 2.16 kg at 190°C.

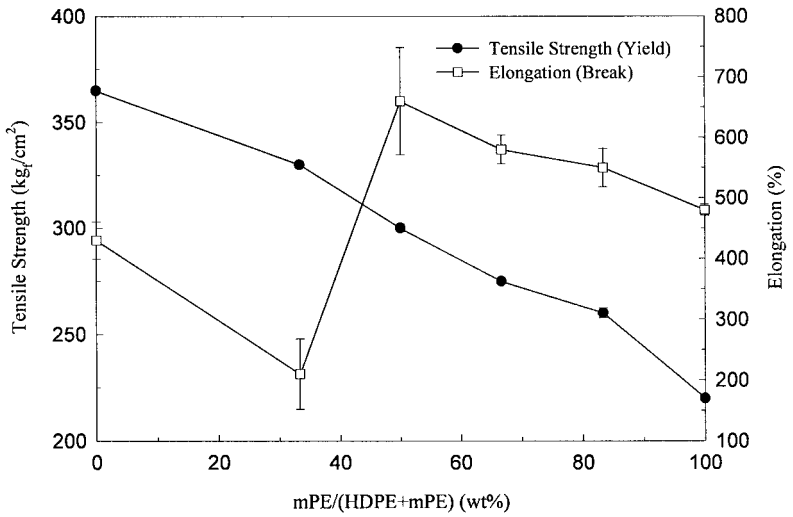

Figure 12 Tensile strength at yield and elongation at break versus HDPE/mPE binary blend composition in PP/mPE/HDPE ternary blends.

than 33.3 wt % at room temperature and 16.7 wt % at 0°C of HDPE/mPE blend.

Izod impact strength, tensile strength, and elongation at break increased abruptly between 15 and 20 wt % of mPE in ternary blends, indicative of phase inversion of HDPE/mPE binary blends. When the matrix of the dispersed phase in ternary blend is mPE, the mechanical properties of PP/mPE/HDPE ternary blends are higher than those of the HDPE matrix of dispersed phase. This implies that the compatibility between PP and mPE is better than that of PP and HDPE.

Based on the mechanical properties, antagonistic effects are increased with increasing the collision probability of PP and HDPE, and synergistic effects are increased with increasing the collision probability of PP and mPE in PP/mPE/HDPE ternary blend systems.

CONCLUSIONS

For HDPE/mPE binary blends, the η^* composition curves exhibited PNDB at 0.1–10 rad/s range, NBD at 100 rad/s, and simple additive rule at 398.1 rad/s. Young's modulus and yield strength showed monotonically decreasing NDB with mPE content. The elongation–composition curve showed PNBD with a sharp increment between 33.3 and 50 wt % of mPE. We can conclude that the HDPE/mPE binary blend has phase inversion between 50 and 66.7 wt % mPE and is immiscible in both the melt and solid state.

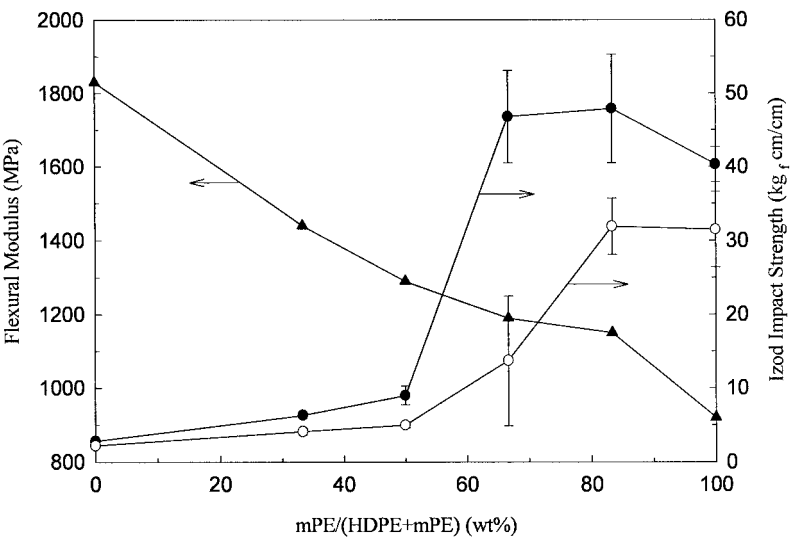

Figure 13 Flexural modulus and Izod impact strength (at 0 and 23°C, with notched) versus HDPE/mPE binary composition in PP/mPE/HDPE ternary blends. Open circles and filled circles are Izod impact strength, at 0 and 23°C, respectively.

For PP/mPE/HDPE ternary blends, the η^* composition curves, having a minimum at PHE-25, exhibited NDB over the entire frequency range. Yield strength and hardness showed PDB, whereas elongation at break, flexural modulus, and impact strength showed PNDB with inflection point at about 50 wt % mPE, consistent with the phase inversion point of HDPE/mPE binary blends. The synergistic effects of mechanical properties of PP/mPE/HDPE ternary blends such as tensile strength at break, elongation at break, and impact strength were achieved with the addition of $<$30 wt % HDPE on PP/mPE binary blends.

The PP/mPE/HDPE ternary blend is greatly affected by varying HDPE/mPE composition and is immiscible at melt and miscible above the phase inversion point of HDPE/mPE binary blends.

This research was supported by Pusan National University.

References

1. Paul, D. R.; Newman, S. Polymer Blends; Academic Press: New York, 1978.
2. Paul, D. R.; Bucknall, C. B. Polymer Blends; Wiley: New York, 2000.
3. Jang, B. Z.; Uhlmann, D. R.; Vander Sande, J. B. Polym Eng Sci 1985, 25, 643.
4. De, S. K.; Bhowmic, A. K. Thermoplastic Elastomers from Rubber-Plastic Blends; Ellis Horwood: Chicester, UK, 1990.
5. D'Orazio, L.; Mancarella, C.; Martuscelli, E.; Sticotti, G. J Mater Sci 1991, 26, 4033.
6. Xanthos, M.; Tan, V.; Ponnusamy, A. Polym Eng Sci 1997, 37, 1102.
7. Van der Wal, A.; Verheul, A. J. J.; Gaymans, R. J. Polymer 1999, 40, 6057.
8. Van der Wal, A.; Nijhof, R.; Gaymans, R. J. Polymer 1999, 40, 6031.
9. D'Orazio, L.; Greco, R.; Mancarella, C.; Martuscelli, E.; Ragosta, G.; Silvestre, C. Polym Eng Sci 1982, 22, 536.
10. Yang, D.; Zhang, B.; Yang, Y.; Fang, Z.; Sun, G.; Feng, Z. Polym Eng Sci 1984, 24, 612.
11. Gupta, A. K.; Purwar, S. N. J Appl Polym Sci 1985, 30, 1777.
12. Choudhary, V.; Varma, H. S.; Varma, I. K. Polymer 1991, 32, 2541.
13. Thamm, R. C. Rubber Chem Technol 1977, 50, 24.
14. D'Orazio, L.; Greco, R.; Martuscelli, E.; Ragosta, G. Polym Eng Sci 1983, 23, 489.
15. Stehling, F. C.; Huff, T.; Speed, C. S.; Wissler, G. J Appl Polym Sci 1981, 26, 2693.
16. Utracki, L. A.; Kamal, M. R. Polym Eng Sci 1982, 22, 96.
17. Han, C. D. Multiphase Flow in Polymer Processing; Academic Press: New York, 1981.
18. Wisniewski, C.; Marin, G.; Monge, P. Eur Polym Mater 1985, 21, 479.
19. Valenza, A.; Acierno, D. Eur Polym Mater 1994, 30, 1121.
20. Montfort, J. P.; Martin, G.; Arman, J.; Monge, P. Polymer 1978, 19, 277.
21. Graebling, D.; Muller, R.; Palierne, F. Macromolecules 1993, 26, 320.
22. Han, C. D.; Kim, J. J Polym Sci Part B: Polym Phys 1987, 25, 1741.
23. Wu, S. J Appl Polym Sci 1988, 35, 549.